Bioorganic Chemistry 93 (2019) 103329

Contents lists available at ScienceDirect

Bioorganic Chemistry

journal homepage: www.elsevier.com/locate/bioorg

Synthesis, characterization, anti-proliferative properties and DNA binding of benzochromene derivatives: Increased Bax/Bcl-2 ratio and caspase-dependent apoptosis in colorectal cancer cell line

Mina Hanifeh Ahagh[a], Gholamreza Dehghan[a,*], Maryam Mehdipour[a], Reza Teimuri-Mofrad[b], Elmira Payami[b], Nader Sheibani[c], Maryam Ghaffari[a], Milad Asadi[d]

[a] Department of Biology, Faculty of Natural Sciences, University of Tabriz, Tabriz, Iran
[b] Department of Organic and Biochemistry, Faculty of Chemistry, University of Tabriz, Tabriz, Iran
[c] Department of Ophthalmology and Visual Sciences, Cell and Regenerative Biology, and Biomedical Engineering, University of Wisconsin, School of Medicine and Public Health, Madison, WI, USA
[d] Immunology Research Center, Tabriz University of Medical Sciences, Tabriz, Iran

ARTICLE INFO

Keywords:
Apoptosis
Bcl-2
Benzochromene derivative
Calf thymus DNA
Caspase-3
Groove binding
HT-29 cells

ABSTRACT

3-Amino-1-aryl-1H-benzo[*f*]chromene-2-carbonitrile derivatives were synthesized from three-component reaction of arylaldehyde, malononitrile and 2-naphthol in the presence of 1, 4-bis(4-ferrocenylbutyl)piperazine as a new catalyst. Cytotoxic potencies of the compounds were tested on HT-29 cells. 3-Amino-1-(4-fluorophenyl)-1*H*-benzo[*f*]chromene-2-carbonitrile (**4c**) was more active among these compounds and was selected for further studies. Apoptosis was investigated by acridine orange/ethidium bromide (AO/EtBr) double staining and flow cytometry. The qRT-PCR was used to analyze the expression of pro- and anti-apoptotic genes. The binding attributes of **4c** with calf thymus DNA (ctDNA) was examined using multi-spectroscopic measurements. We found that **4c** had potent cytotoxic activity against HT-29 cells with an IC_{50} value of 60 μM through induction of cell cycle arrest in the sub-G1 phase and apoptosis. RT-PCR analysis demonstrated down-regulation of Bcl-2 expression, while the expression of Bax, caspase-3, -8 and -9 genes was up-regulated in HT-29 cells incubated with **4c** compared with control cells. These studies revealed that 4c interacts with DNA through groove binding mode with the intrinsic binding constant (K_b) of 3×10^2 M^{-1}. Thus, **4c** is a valuable candidate for further evaluation as a new series of potent chemotherapeutic family in colon cancer treatment.

1. Introduction

Cancer is one of the harmful diseases, being a primary general health problem as well as a main killer worldwide [1]. At present, colorectal cancer is one of the most important reason of cancer deaths in humans and a great rate of resistance to common chemotherapies has been recorded as a major limitation. Thus, there are increasing attempts to stop the progression of this disease by the application of either new synthetic or natural compounds [2,3]. Anticancer compounds eliminate cells that are immortal either by disturbing cellular pathways that are critical for cell permanence or by way of inducing apoptosis (programmed cell death) [4]. Apoptosis is a gene-regulated phenomenon, that is distinguished by specific structural features, as cell and nuclear shrinkage, formation of plasma membrane blebs, chromatin condensation, and oligonucleosomal DNA fragmentation [5]. Two major molecular ways that trigger programmed cell death include the extrinsic (is initiated by activation of death receptor) and the intrinsic (is activated by cellular stresses) pathways [4].

The extrinsic pathway is associated with controlling cell turnover by eliminating mutant cells. In this pathway, cell death is stimulated by the interplay among death ligands (like TNF) and their appropriate death receptors. The death development initiating complex then induces the activity of caspase-8 and caspase-3, which are the starter and effector caspases, respectively [6,7]. The intrinsic pathway is triggered in response to the antineoplastic drug action that damages DNA and causes the exit of mitochondrial proteins like cytochrome *c* that promotes caspase-9 and caspase-3 activity [6,8]. Also, in the mitochondria mediated pathway, pro- and anti-apoptotic Bcl-2 family members play important roles; the ratio of pro- and anti-apoptotic proteins (e.g. Bcl-2/Bax) is regarded as a determinant of whether a cell will undergo

* Corresponding author.
E-mail address: gdehghan@tabrizu.ac.ir (G. Dehghan).

https://doi.org/10.1016/j.bioorg.2019.103329
Received 7 August 2019; Received in revised form 19 September 2019; Accepted 28 September 2019
Available online 30 September 2019

apoptosis or survive [9]. Various studies have shown that the excessive levels of anti-apoptotic Bcl-2 family members consisting Bcl-2, Bcl-xl, Mcl-1, Bcl-w play a significant role in resistance of tumor cells to chemotherapy. Thus, a decrease in Bcl-2 and an increase in Bax expression can induce the apoptotic process and eliminate cancer cells [10].

With regard to chemotherapeutic drugs causing cell death, there are increasing attempts towards development of anti-Bcl2 compounds to induce apoptosis. The chromene derivatives are recently reported as a new effective anti-tumor compounds [11,12].

Chromenes (benzopyrans) are attracting widespread interest due to their various biological potentials. Heterocyclic compounds like benzochromens have many roles in the progress of present pharmaceuticals, typical resources, agriculture productions and dyes. Many publications have appeared in recent years demonstrating that most chemotherapeutic compounds stimulate apoptosis as a mode of cell death in cancer cells [13,14]. Global statistics display that the annual rate of cancer is rising and that is required to model new integrated heterocyclic moieties to produce potential anticancer drugs with helpful biological uses. They are heterocyclic ring system, including a pyran ring combined with benzene ring. Benzopyran forms the basic scaffold of different types of polyphenols and obtained in natural tocopherols, anthocyanins, alkaloids, flavonoids and it can be also found in tannins, tea, fruits and vegetables [14]. Chromenes and their derivatives scaffolds of dihydropyranochromene are one of the most commonly encountered oxygen containing heterocycles [15,16] have a wide span of biological properties, including anti-cancer [17,18], antimicrobial activities [19,20], anti-inflammatory effects [21] antioxidant [22], antiviral, anti-HIV, anti-lishmanial, and anti-anaphylactic activities [23]. Also, chromene derivatives can be effected the therapy of neurodegenerative diseases, as amyotrophic lateral sclerosis, Parkinson's disease, Alzheimer's disease, Down's syndrome, AIDS associated dementia and treatment of schizophrenia and myoclonus [16,19]. The application of different chromene systems with potential candidates that can be used as drug targets for cancer treatment has been reported in several types of cancer cell treatment. For example, the 2-amino-7-dimethylamino-4-aryl-4*H*-chromene-3-carbonitrile displayed growth inhibition of the multidrug-resistant human uterine sarcoma (MES-SA/DX-5) [24]. Moreover, 1*H*-benzo[*f*]chromene derivatives have displayed as one of the most auspicious and desirable scaffolds for the development of potent antitumor agents. For example, several derivatives of 1*H*-benzo[*f*]chromene, compounds showed promising cytotoxic and apoptotic effects on various cancer cell lines [25,26]. On the other hand, the 7H-benzo[*h*]chromeno [2,3-*d*] pyrimidine derivative exhibited significantly more potent antitumor activity against different human cancer cell lines [27]. And, the cytotoxic activities of the 2-amino-4-aryl-3-cyano-7- (dimethylamino)-4*H*-chromenes against six human tumor cell lines were evaluated [12].

Lately owing to the spread of cancer disease, there has been an increasing attention to studying the interaction of small molecules with DNA as anti-cancer drugs. The small molecules apply their anticancer activities by binding to DNA, thereby damaging DNA structure, changing replication of double helix DNA, hindering the division of cancer cell, also leading to cell. Small molecules binds to DNA through covalent and/or non-covalent interactions [28,29] such as electrostatic binding for cations, intercalative binding with planar ligands, and groove binding with some other ligands [16,30]. In continuation of our previous researches on the synthesis of ferrocene derivatives [31] and the modification of the multicomponent reactions with these type of compounds [32,33], in the present study, we report a new catalyst that contains ferrocene moiety as an efficient available catalyst for the synthesis of 3-amino-1-aryl-1*H*-benzo[*f*]chromene-2-carbonitrile derivatives according to three-component reaction of arylaldehyde, malononitrile and 2-naphthol. The *in vitro* cytotoxic activity of **4c** (Fig. 1) was determined using MTT assays, assessment of cell death based on morphological features and flow cytometry assessments of apoptosis in human HT-29 cells. Also, we studied the relationship of a chemotherapeutic efficacy to Bcl-2 and Bax gene expression as well as activation of caspase-3, -8 and -9. Also, the interaction properties of **4c** with double helix DNA were recorded by UV–Vis absorption and fluorescence spectroscopy and viscosity measurements.

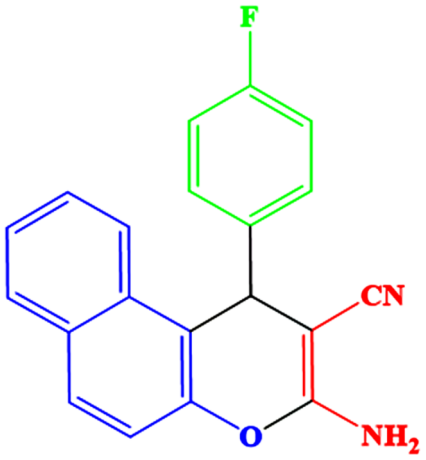

Fig. 1. Structure of cells 3-Amino-1-(4-fluorophenyl)-1*H*-benzo[*f*]chromene-2-carbonitrile (**4c**).

2. Materials and methods

2.1. Chemistry

All chemical reagents used in our experiments were purchased from Sigma-Aldrich and Merck companies. Experimental section melting points were determined in open capillaries with a MEL-TEMP model 1202D apparatus. FT-IR spectra were recorded from KBr disk on the FT-IR Bruker Tensor 27 spectrometer. ^{1}H and ^{13}CNMR spectra were recorded with a Bruker Spectrospin Avance 400 spectrometer. The elementary analyses were carried out by Vario EL III analyzer.

2.1.1. Synthesis and characterization of 1, 4-bis(4-ferrocenylbutyl) piperazine as catalyst

A 50 ml round-bottom flask equipped with a reflux condenser was charged with 4-chlorobutylferrocene (0.61 g, 2.2 mmol), piperazine (0.086 g, 1 mmol), sodium carbonate (0.17 g, 1.6 mmol) and acetonitrile (25 ml) and the mixture was refluxed for 48 h, after this period, the reaction mixture was diluted with water and extracted with dichloromethane (3 × 30 ml). The combined organic phases were dried over Na_2SO_4 and evaporated on a rotary evaporated under atmospheric pressure. The crude product was purified by column chromatography (methanol/ethyl acetate, 1:9) and the desired product was obtained in 87% yields.

0.49 g of orange solid was obtained (m.p. 98–100 °C). FT-IR (KBr, cm^{-1}): 3082 (C—H Ar), 2930, 2803 (C—H), 1634, 1530 (C=C), 1111, 998 (C—N), 486 (Cp-Fe); ^{1}H NMR (400 MHz, CDCl3): δ 1.51 (m, 8H, $CH_2CH_2CH2CH_2$), 2.34 (m, 4H, Cp-CH2, 2.51 (br, 12H, NCH_2), 4.02–4.04 (m, 8H, $CpCH_2$-), 4.08 (s, 10H, Cp); ^{13}C NMR (100 MHz, CDCl3,): δ 25.5, 27.9, 28.4, 51.9, 57.4, 66.0, 66.9, 67.4, 88.0. Elemental analysis: calcd for $C_{32}H_{42}Fe_2N_2$ (%): C 67.27, H 7.40, N 4.90, Fe 20.43.

Found (%): C 67.42, H 7.32, N 4.81, Fe 20.51.

*2.1.2. General procedure for synthesis of 3-amino-1-aryl-1H-benzo[f] chromene-2-carbonitrile derivatives (**4a-f**)*

To a mixture of 2-naphthol (1 mmol), appropriate arylaldehyde (1 mmol) and malononitrile (1.2 mmol), 10 mg of 1, 4-bis(4-ferrocenylbutyl) piperazine was added as catalyst. The reaction mixture was stirred at 100 °C in an oil bath under solvent free condition. After completion of the reaction (monitored by TLC), the reaction mixture was cooled and the obtained precipitate was washed with dichloromethane. Finally, the material was recrystallized from ethanol.

2.1.3. Selected spectral data

*2.1.3.1. 3-Amino-1-phenyl-1H-benzo[f]chromene-2-carbonitrile (**4a**)*. White solid. m. p. 278–280 °C ^{1}HNMR (400 MHz, DMSO-d_6): δ 5.29 (1H, s, CH), 6.99 (2H, s, NH_2), 7.12–7.27 (5H, m, Ar-H), 7.33–7.35 (1H, d, J = 8.91 Hz, Ar-H), 7.38–7.45 (2H, m, Ar-H), 7.82–7.84 (1H, m, Ar-H), 7.89–7.94 (2H, m, Ar-H) ppm.

*2.1.3.2. 3-Amino-1-(4-methoxyphenyl)-1H-benzo[f] chromene-2-carbonitrile (**4d**)*. White solid. m. p. 191–193 °C ^{1}H NMR (400 MHz, DMSO-d_6): δ 3.65 (3H, s, OCH_3), 5.24 (1H, s, CH), 6.79–6.81 (2H, d, J = 8.49 Hz, Ar-H), 6.94 (2H, s, NH_2), 7.09–6.11 (2H, d, J = 8.56 Hz, Ar-H), 7.31–7.32 (2H, d, J = 8.93 Hz, Ar-H), 7.38–7.45 (2H, m, Ar-H), 7.83–7.85 (1H, d, J = 7.93 Hz, Ar-H), 7.89–7.92 (2H, m, Ar-H) ppm.

*2.1.3.3. 3-Amino-1-(thiophen-2-yl)-1H-benzo[f]chromene-2-carbonitrile (**4f**)*. Yellow solid. m.p. 257–259 °C ^{1}HNMR (400 MHz, DMSO-d_6): δ 5.71 (1H, s, CH), 6.86–6.88 (1H, m, Ar-H), 7.01 (1H, d, J = 2.90 Hz, Ar-H), 7.14 (2H, s, NH_2), 7.24–7.26 (1H, m, Ar-H), 7.30 (1H, d, J = 8.93 Hz, Ar-H), 7.42–7.45 (1H, m, Ar-H), 7.48–7.52 (1H, m, Ar-H), 7.90–7.93 (2H, m, Ar-H), 8.03 (1H, d, J = 8.38 Hz, Ar-H) ppm.

2.2. Biological activities

The cell culture medium (RPMI 1640), fetal bovine serum (FBS) and penicillin-streptomycin were obtained from Gibco (life technologies, Paisley, Scotland). The culture plates were purchased from Nunc (Kamstrupvej, Denmark). Annexin-V FITC apopotosis kit was obtained from Roche (Mannheim, Germany). Dimethylsulfoxide (DMSO), Tris-HCl, ethidium bromide (EtBr), propidium iodide (PI), MTT assay kit, acridine orange (AO), and Calf thymus DNA (ctDNA) were obtained from Sigma-Aldrich (St. Louis, MO, USA). The human HT-29 cell line was purchased from Pasteur Institute of Iran (Tehran, Iran).

2.2.1. Cell culture

The human HT-29 cancer cells were cultured in a cell culture medium and added 10% fetal bovine serum, 100 IU/ml penicillin and 100 μg/ml streptomycin. The HT-29 cells were incubated at 37 °C under a 5% CO_2 atmosphere [34].

2.2.2. Cytotoxicity of chromene derivatives

MTT (water soluble tetrazolium salt assay) is an assay to specify viability of cells with the changing of the water-soluble tetrazolium salt to an unsolvable purple formazan by respiring cells. HT-29 cells (4×10^4 cells/well) were pipetted into 96-well cell culture plates for 24 h before to adding **4a-f** and were incubated at 37 °C and 5% CO_2. After treatments with **4c**, at different doses for various time intervals, 20 μL of the tetrazolium salt (5 mg/ml in PBS) stock solution were added to each plate and maintained for 3 h. During maintenance, 200 μL of Dimethylsulfoxide was added to disperse the dissoluble crystals and the absorbance was recorded at 570 nm by a plate reader [35].

2.2.3. Morphological assessment of the apoptotic cells

To study the effect of **4c** on apoptosis, the cells were stained using fluorescent acridine orange/ethidium bromide (AO/EtBr). For morphological analysis, HT-29 cells (5×10^5 cells/well) were pipetted into 6 wells, and maintained with the respective IC_{50} concentration of **4c** for 24 and 48 h. The HT-29 Cells were washed with 200 μL of cold phosphate-buffered saline (PBS). Cells (10 μL) were put on a glass slide and mixed with the AO/Et Br stock solution (1:1, v/v) at a ultimate concentration of 100 μg/m. Samples were examined by fluorescence microscopy (Olympus BX 41, Hamburg, Germany) [36].

2.2.4. Cell cycle study

Flow cytometry method was applied to study the apoptosis and cell cycle dispersal of HT-29 cells incubated with **4c** at IC_{50} concentration. The HT-29 cells (5×10^5 cells/well) were pipetted into 24 wells for 24 h earlier to incubation with 60 μM of **4c** for 24 and 48 h. Later HT-29 cells were gathered and stained with 70% cold ethanol and maintained at −20 °C for 30 min. Following the incubation, cells were collected, suspended with PBS, and dyed with 1 mg/mL propidium iodide (PI) and 10 mg/mL RNase and maintained in dark room temperature for 15 min. Finally, cell cycle distribution was recorded by flow cytometry. The fraction of HT-29 cells in the sub-G1, G0/G1, S and G2/M phases were evaluated by Multicycle Cell Cycle software (Partec PAS, Munster, Germany) [37,38].

2.2.5. Annexin-V-FITC/PI double staining assays

To further verify cell death, Annexin V/PI staining was utilized to detect the localization of phosphatidyl serine (PC) on the outside of the cell membrane [39]. Annexin-V/PI staining allows the quantitative determination of apoptotic cells on a single-cell basis using flow cytometry. HT-29 cells (5×10^5 cells/well) were seeded in 24 well cell culture plates for 24 h, and then incubated with the respective IC_{50} concentration of **4c** for 24 and 48 h. Following collection, the cells were suspended with PBS, re-suspended in Annexin binding buffer (10 mM HEPES/NaOH, pH 7.4, 140 mM NaCl, 2.5 mM $CaCl_2$), and 10 μL of Annexin-V FITC and 10 μL PI (according to the manufacture's recommendations) were added. The HT-29 cells were kept in the covert area for 30 min, and studied by flow cytometry (Partec PAS) [4,40].

2.2.6. Evaluation of Bax and Bcl-2 gene expression upon 4c treatment

Total RNA was prepared from treated and untreated cells using Tripure isolation reagent (Roche, Cat No. 11667165001) based on the protocol and stored at −80 °C. The cDNA was prepared using TAKARA complementary DNA synthesis kit (TAKARA, Cat No. 6130). SYBR green PCR master mix (TAKARA, Cat No. RR820W) and primer set for each gene (Table 1) were used for qPCR. GAPDH (housekeeping gene) expression level was utilized for normalization. Finally, the mean of duplicated C_t values was determined and the relative expression level of Bax, Bcl-2 and caspase-3, -8 and -9 genes were calculated by the comparative C_t method.

2.2.7. DNA binding experiments

2.2.7.1. Preparation of stock solution. A stock solution of **4c** was prepared by dissolution a proper quantity of **4c** in Tris-HCl buffer containing 0.3% DMSO. The ctDNA stock solution was made by dispersing a proper quantity of ctDNA in Tris-HCl buffer (10 mM, pH 7.4) and stored at 4 °C. A solution of ctDNA presented a proportion of

Table 1
Primer sequences and their specifications used in quantification real-time PCR.

Gene	Sequences
Bax-F	5′-CGACGGCAACTTCAACTGGG-3′
Bax-R	5′-CCCATGATGGTCCTGATCAACT-3′
Bcl-2-F	5′-GAGCGTCAACAGGGAGATGTC-3′
Bcl-2-R	5′-TGCCGGTTCAGGTACTCAGTC- 3′
Caspase-3-F	5′-ATGGTTTGAGCCTGAGCAGA-3′
Caspase-3-R	5′-GGCAGCATCATCCACACATAC-3′
Caspase-8-F	5′-ACCTTGTGTCTGAGCTGGTCT-3′
Caspase-8-R	5′-GCCCACTGGTATTCCTCAGGC-3′
Caspase-9-F	5′-GCAGGCTCTGGATCTCGGC-3′
Caspase-9-R	5′-GCTGCTTGCCTGTTAGTTCGC-3′
GAPDH-F	5′-CAAGATCATCAGCAATGCCTCC-3′
GAPDH-R	5′-GCCATCACGCCACAGTTTCC-3′

UV absorbance at 260 and 280 nm (A_{260}/A_{280}), which was in the range of 1.8–19, implying that DNA was free from protein. The concentration of double helix DNA was computed spectrophotometrically by ε of 6600 M^{-1} cm^{-1} at 260 nm.

2.2.7.2. UV–Vis absorption spectra. To investigate the interaction between ctDNA and **4c**, the UV–vis spectra were recorded using PG Instrument (T60, PG Instruments Ltd, Leicestershire, UK) spectrophotometer. The absorption spectrum of **4c** was evaluated in the absence or presence of ctDNA for a constant compound concentration and various ctDNA amounts. Also, ctDNA solution spectra was recorded in the absence and presence of the **4c**. The reference solution was Tris-HCl buffer solution.

2.2.7.3. Fluorescence spectroscopy. Fluorescence emission spectra of **4c** was measured using FP6200 JASCO spectrofluorometer (Tokyo. Japan). The emission property of **4c** in the presence of different concentration of ctDNA was determined. The fluorescence quenching measurements were analyzed using a fixed concentration of 4c (1.0×10^{-3} M) and different amounts of ctDNA. Excitation of **4c** was done at 280 nm and emission spectra were documented from 400 nm to 470 nm. Both excitation and emission slit were set at 5 nm. Stern-Volmer equation was applied to obtain the quenching constant values (K_{SV}) both in the absence and presence of ctDNA.

2.2.7.4. Viscosity measurement. To further study the bonding properties of **4c** with ctDNA, viscosity measurements was performed by a viscometer (Ubbelohde-Iran) at 25 °C. Double helix DNA solution viscosity was evaluated in the absence or presence of adding different amounts of **4c**. Flow time was computed with a digital stopwatch, taking the mean value of three measurements. The data got were reported as $(\eta/\eta_0)^{1/3}$ versus [compound]/[DNA], where η and η_0 are the viscosity measured for the DNA solution in the presence and absence of **4c**, respectively [41].

2.3. Statistical analysis

The statistical analysis was performed by Graph-Pad Prism 6 (San Diego, CA, USA). All data were revealed as mean ± standard deviation (SD). Statistical importance of differences between groups was analyzed by two-way ANOVA.

3. Results and discussion

3.1. Chemistry

3.1.1. Catalyst investigation

Firstly, in order to investigate the catalyst, we choose the reaction between 2-naphthol (**1**) with benzaldehyde (**2**) and malononitrile (**3**) as a model reaction. Various catalysts were tested in this model reaction under solvent free conditions at room temperature and obtained data were collected in Table 2. As can be seen from the Table 2, in the absence of the catalyst, the desired product yield was low. The results

Table 2
Screening of various catalysts under solvent free conditions for the model reaction.

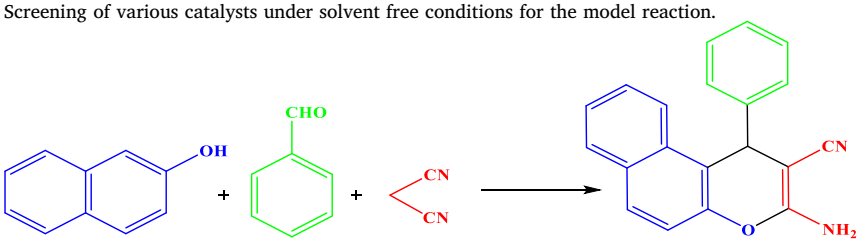

1 **2a** **3** **4a**

Entry	Catalyst	Time (min)	Yield (%)
1	–	120	trace
2	–	120	trace
3	DABCO	90	15
4	CH_3COOH	90	12
5	Na_2SO_4	90	8
6	MgO	90	8
7	H_2SO_4	90	10
8	p-TSA	90	10
9	1-methyl-4-(ferrocenylbutyl)piperazine	90	30

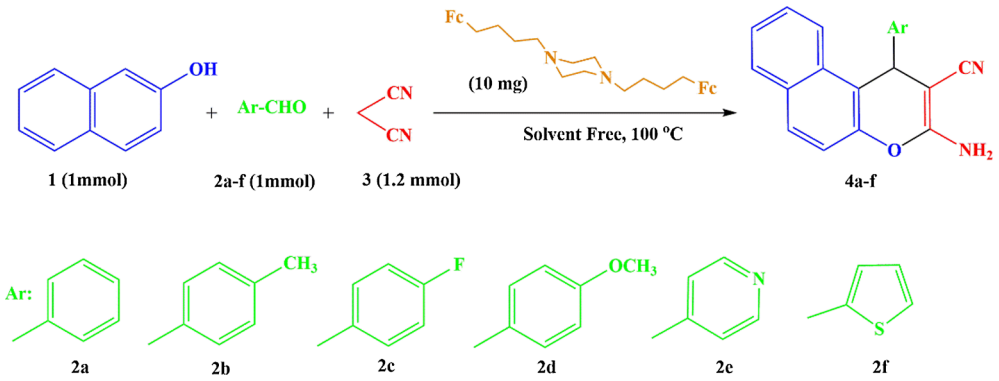

Scheme 1. Synthesis of various cells 0.3-amino-1-aryl-1*H*-benzo[*f*]chromene-2-carbonitrile derivatives (**4a-f**) under optimized conditions.

Table 3
Optimization of the reaction conditions such as solvent, temperature, time, and amount of synthesized catalyst in the model reaction.[a]

Entry	Catalyst amount (mg)	Solvent	Temperature (°C)	Time (min)	Yields (%)
1	50	H_2O	r.t.	90	15
2	50	EtOH	r.t.	90	17
3	50	$CHCl_3$	r.t.	90	12
4	20	–	r.t.	80	23
5	10	–	r.t.	80	25
6	5	–	r.t.	80	18
7	10	–	60	60	42
8	10	–	70	60	48
9	10	–	80	50	45
10	10	–	90	40	60
11	10	–	100	35	75

[a] Reaction conditions: 2-naphthol/benzaldehyde/malononitrile = 1:1:1.2

indicated that the yields were improved by using the catalyst in the model reaction. Various conventional acidic and basic catalysts afforded the desired product in low yields. In contrast to the conventional catalyst, the synthesized catalyst, [1-methyl-4-(ferrocenylbutyl)piperazine] [31], containing ferrocene moiety as a Lewis acid and amine moiety as a Lewis base led to a better yield (30%). In continuation, we were designed, synthesized and used the new ferrocene based catalyst (Scheme 1) in this multicomponent reaction for the synthesis of 3-amino-1-aryl-1*H*-benzo[*f*]chromene-2-carbonitrile derivatives (**4a-f**).

In order to optimize the reaction conditions, different conditions such as various solvents, temperatures, times, and amount of catalyst were used and the obtained results were summarized in Table 3. As shown in Table 3, better result (75% yield) was achieved when the reaction was carried out using 10 mg of catalyst at 100 °C reaction temperature under solvent free condition (Entry 11).

After optimization of the reaction conditions, various derivatives of 3-amino-1-aryl-1*H*-benzo[*f*]chromene-2-carbonitrile (**4a-f**) (Scheme 1) were synthesized using 10 mg of catalyst at 100 °C under solvent-free conditions (Table 4). After the completion of the reaction, the obtained precipitate was washed several times with dichloromethane until the filtrate was colorless and the residue was recrystallized from ethanol to afford the desired product. In fact, this synthesized ferrocene based catalyst has several acid and base sites that they acted as active sites of the catalyst (Fig. 2). Hence, these active sites can be promoted the reaction.

3.2. Biological activities

3.2.1. Anti-proliferative and apoptotic activity

Cell viability and IC_{50} values of benzochromene derivatives (**4a-f**) was determined using MTT assays. Cell viability was investigated following the treatment of various concentration of compounds. The IC_{50} values of the benzochromene derivatives (**4a-f**) are shown in Table 5 was investigated after 72 h by water soluble tetrazolium salt (MTT) assay. The results showed that some of the synthesised compounds exhibited superior to modest anti-proliferative activity against HT-29 cells. In particular, compound **4c** was displayed the most potent counterparts, as it was more active others. Furthermore, as shown in Table 5, compounds **4a**, **4b**, **4c**, **4d**, **4e** and **4f** with the IC_{50} values of 112 μM, 90 μM, 60 μM, 78 μM, 83 μM and 71 μM, respectively, were evaluated. The IC_{50} values (amount of **4c** that causes a 50% decrease in cell viability) of **4c** with 60 μM (Fig. 3A) was more active against HT-29 cells. These results indicated that **4c** reduced cell proliferation of the treated HT-29 cells in a dose and time-dependent manner [42,43]. The results presented in Fig. 3B, indicated that cisplatin caused significant decrease in cell viability of HT-29 as compared to **4c**. The IC_{50} value of cisplatin on HT-29 cells was found to be 39 μM. These values are in good agreement with recent studies that showed the cytotoxicity of different benzochromene derivatives on various types of cancer cells, like human liver cancer, human cervical cancer, and human leukemia [43]. The treatment of HT-29 cells with conferone (2*H*-chromene) was showed a profound decrease in cell viability both dose- and time-dependently [2]. In another study, cytotoxic activity of 1*H*-benzo[*f*] chromene derivatives were investigated against a group of three human cancer cell lines [44]. **4c** was selected for more studies to investigate the mechanism of cell death.

To detect the induction of apoptosis, HT-29 cells were seeded and incubated with indicated concentrations (IC_{50} value = 60 μM) of the **4c** for 24 and 48 h. The cells were then stained with the fluorescent DNA binding dyes (AO/EtBr) to discern the apoptotic cells. Microscopic observations indicated that all the nuclei in untreated cells showed a usual spherical structure and chromatin organization. In contrast, the cells incubated with **4c** were characterized by chromatin condensation and fragmentation, a trait of apoptotic cells. The necrotic cells show identically orange-stained cell nuclei with no condensed chromatin. As shown in Fig. 4, the live cells had normal green nucleus, but apoptotic cells exhibited bright green dots in their nuclei with chromatin condensation or fragmentation. These results revealed that **4c** has pro-apoptotic effects on HT-29 cancer cells.

Table 4
Synthesis of 3-amino-1-aryl-1*H*-benzo[*f*]chromene-2-carbonitrile derivatives (**4a-f**) under optimized conditions.

Entry	Product	Time (min)	Yield (%)	Obs. m.p. (°C)	Lit. m.p. (°C)
1	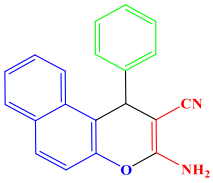	35	78	278–280	279–280 [67]
2	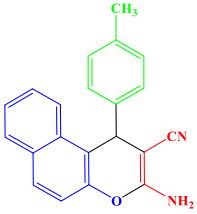	35	75	271–273	273–274 [67]
3	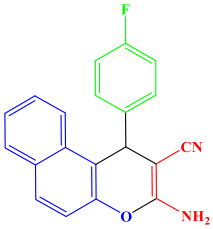	25	70	230–233	228–229 [67]
4	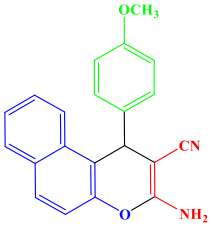	35	64	191–193	190–192 [67]
5	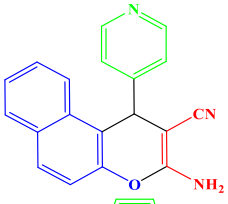	40	54	226–228	227–229 [67]
6	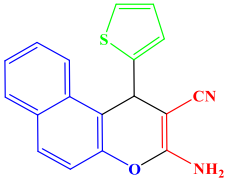	40	50	257–259	258–260 [31]

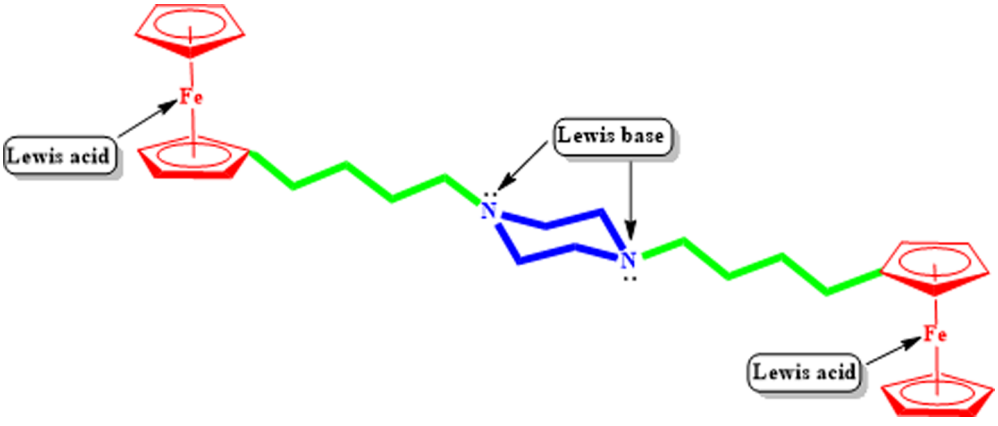

Fig. 2. Various active sites in the novel synthesized catalyst.

Table 5
The IC_{50} values of investigated benzochromen compounds after 72 h of exposure. Each value represents the means of three independent experiments ± S.D. ($P < 0.05$).

Compound	Compound name	IC_{50} (μM)
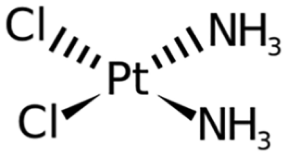	**Cisplatin** 39	
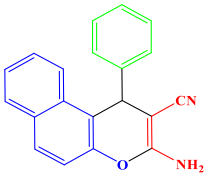	**4a**	112
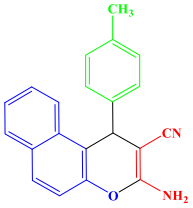	**4b**	90
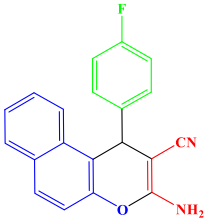	**4c**	60
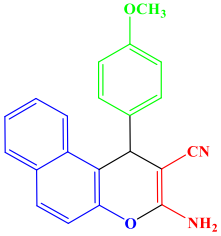	**4d**	78
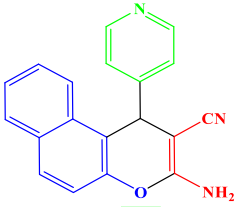	**4e**	83
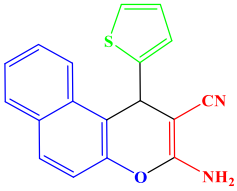	**4f**	71

3.2.2. Flow cytometry detection of apoptotic cells

Flow cytometry method was applied to detect the cell dispersal in varying phase of the cell cycle, and explored whether **4c** could induce apoptosis. Fig. 5 displays the part of cells was increased in the sub-G1 phase following incubation of HT-29 cells with **4c**. The cell cycle dispensation of untreated cells was included in sub-G1, G0/G1, S and G2/M phase by about 12.22%, 57.04%, 10.06% and 17.13%, respectively. Whereas, the cell cycle distribution for HT-29 cells after treatment for 24 and 48 h were 36.95%, 40.33%, 7.00%, 15.72% and 46.91%, 30.33%, 9.33% and 9.88%, at sub-G1, G0/G1, S and G2/M phase, respectively. These results indicated that **4c** induced sub-G1phase arrest and apoptosis in HT-29 cells. Cheraghi and coworkers showed that natural coumarin conferone attributed a robust increase in the number of HT-29 cells at G0/G1 phase that implied cell arrest at G0/G1 phase [2].

To more confirm apoptosis, we used a flow cytometry method based on the exposure of phosphatidyl serine (PS) on the cell surface by Annexin V-FITC/PI double staining, a simple marker of apoptosis induction [45]. This test is used to separate between live cells ($FITC^-/PI^-$), early apoptotic cells ($FITC^+/PI^-$), late apoptotic cells ($FITC^+/PI^+$), and necrotic cells ($FITC^-/PI^+$) [46]. The lower left quadrant of the diagram represents the viable cells, which exclude FITC and PI. The upper right quadrant displays the non-viable necrotic cells, positive for FITC and showing PI uptake. The lower right quadrant shows the apoptotic cells, FITC positive and PI negative, indicating Annexin V binding and cytoplasmic membrane integrity. Fig. 6 displays that incubation of HT-29 cells with **4c** for 24 and 48 h resulted in a cell population shifts from early to late apoptosis or necrosis compared with untreated HT-29 cells. Furthermore, the percentage of cells in early and late apoptosis was assessed for 24 h to be 3.71%, 22.88% and 48 h to be 4.16%, 47.29%, respectively. Naseri and coworkers showed that 4-aryl-4*H*-chromenes induce apoptosis in HepG2, T47D and HCT116 cells. As compound after 72 h propelled > 60% of HepG2 and T47D and > 70% of HCT116 cells into die via apoptosis [47].

3.2.3. Over- expression and down- expression of apoptosis-related genes in HT-29 cells

For further assessment, activation of Bcl-2, Bax, caspase-3, -9 and -8, which play important roles in the initiation and execution of apoptosis were analyzed. Impaired apoptosis acts a significant function in development of cancer cells and restricting the effectiveness of cancer therapies [48,49]. Thus, the induction of apoptosis is a logical way to reduce cell proliferation. Even so, cancer cells have grown different strategies to oppose apoptotic cell death [50]. Up-expression of anti-apoptotic Bcl-2 family members is one such strategy, which increases apoptosis resistance. During the intrinsic (mitochondrial) apoptotic pathway, DNA damage as an apoptotic stimuli induces the release of mitochondrial proteins such as cytochrome *c* (Cyt c) and second mitochondria-derived activator of caspases (Smac) from the intermembrane space to the cytosol [51]. Cytochrome *c* promotes activation of initiator procaspase by forming a multimeric complex with other molecules including Apaf-1 and pro-caspase-9, causing caspase-9 and subsequently caspase-3, -6 and -7 activation [52]. A major mammalian apoptotic pathway is that mediated by a group of death receptors in the tumor necrosis factor receptor (TNFR) superfamily, which includes TNFR1, CD95 (Fas/APO-1) and death receptors (DR) 3–6. These receptors play crucial roles in the regulation of immune responses. CD95-mediated apoptosis, for example, is critical for the maintenance of peripheral immune tolerance and the elimination of cells infected by ligands. Upon binding to their corresponding trimeric ligands, these receptors recruit an initiator procaspase, procaspase-8, to the membrane-associated death-inducing signaling complex (DISC). The critical role of caspase-8 in death receptor-mediated apoptosis is underscored by the observation that cells deficient in caspase-8 are resistant to

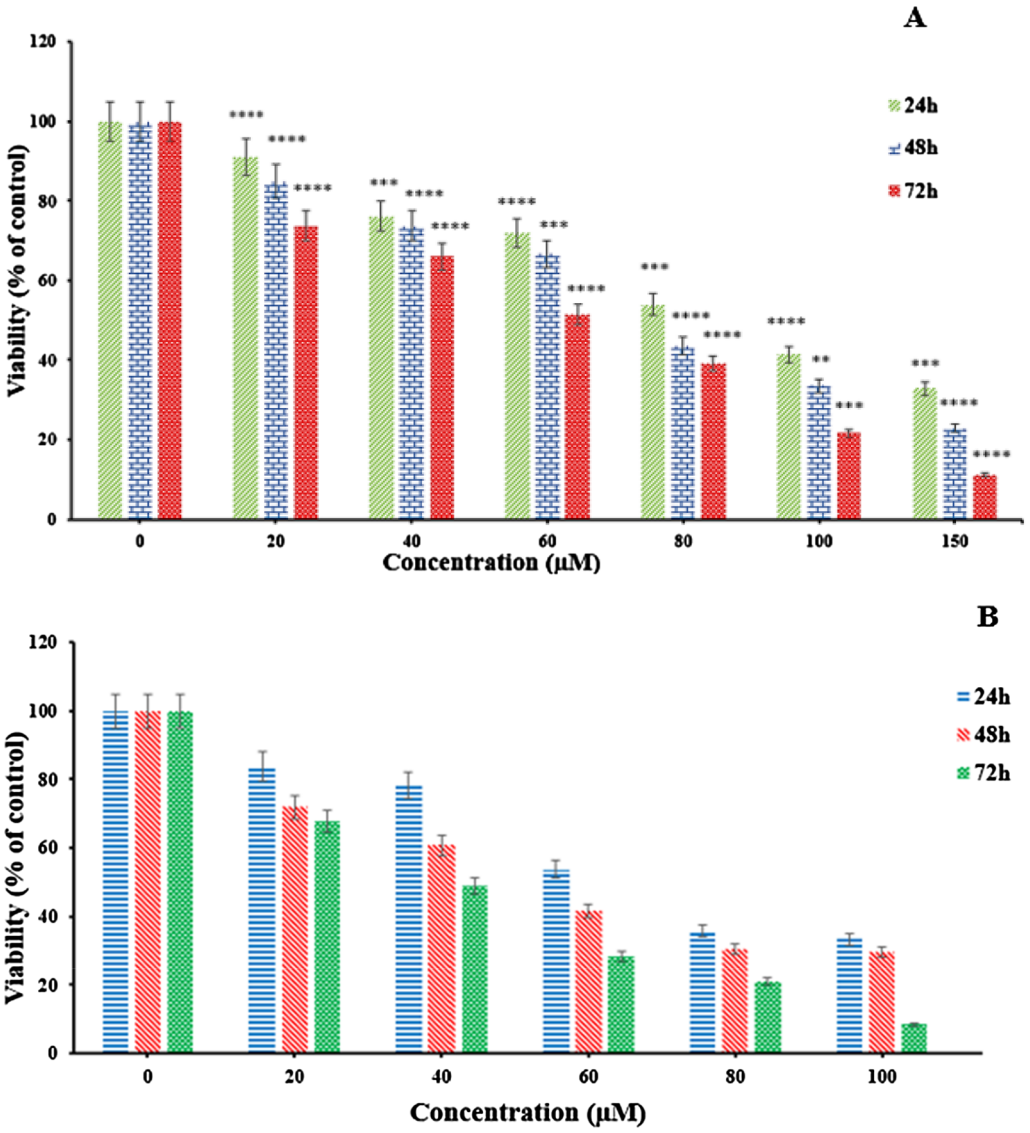

Fig. 3. (A) Antiproliferative effect of **4c** on HT-29 cells. The cells were subjected to various concentrations (20–150 μM) of **4c** for 24, 48 and 72 h. Cell viability was assessed by MTT assay and presented as percentage of the corresponding controls. (B) The cells were treated with various concentrations of cisplatin (20–100 μM). The results are the means of three independent experiments ± S.D. ($P < 0.05$).

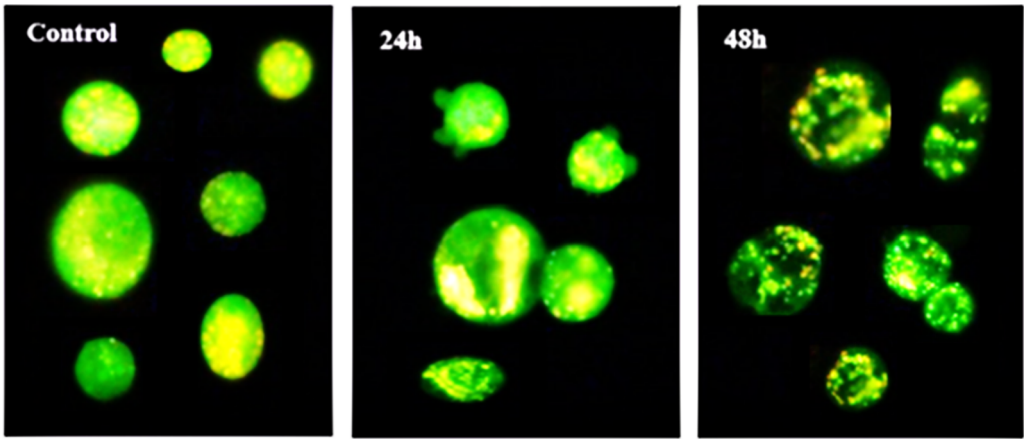

Fig. 4. Morphological changes of the HT-29 cells treated with **4c** by fluorescence microscopy. After treatment with **4c** for 24 and 48 h, the cells were harvested and stained with AO/EtBr.

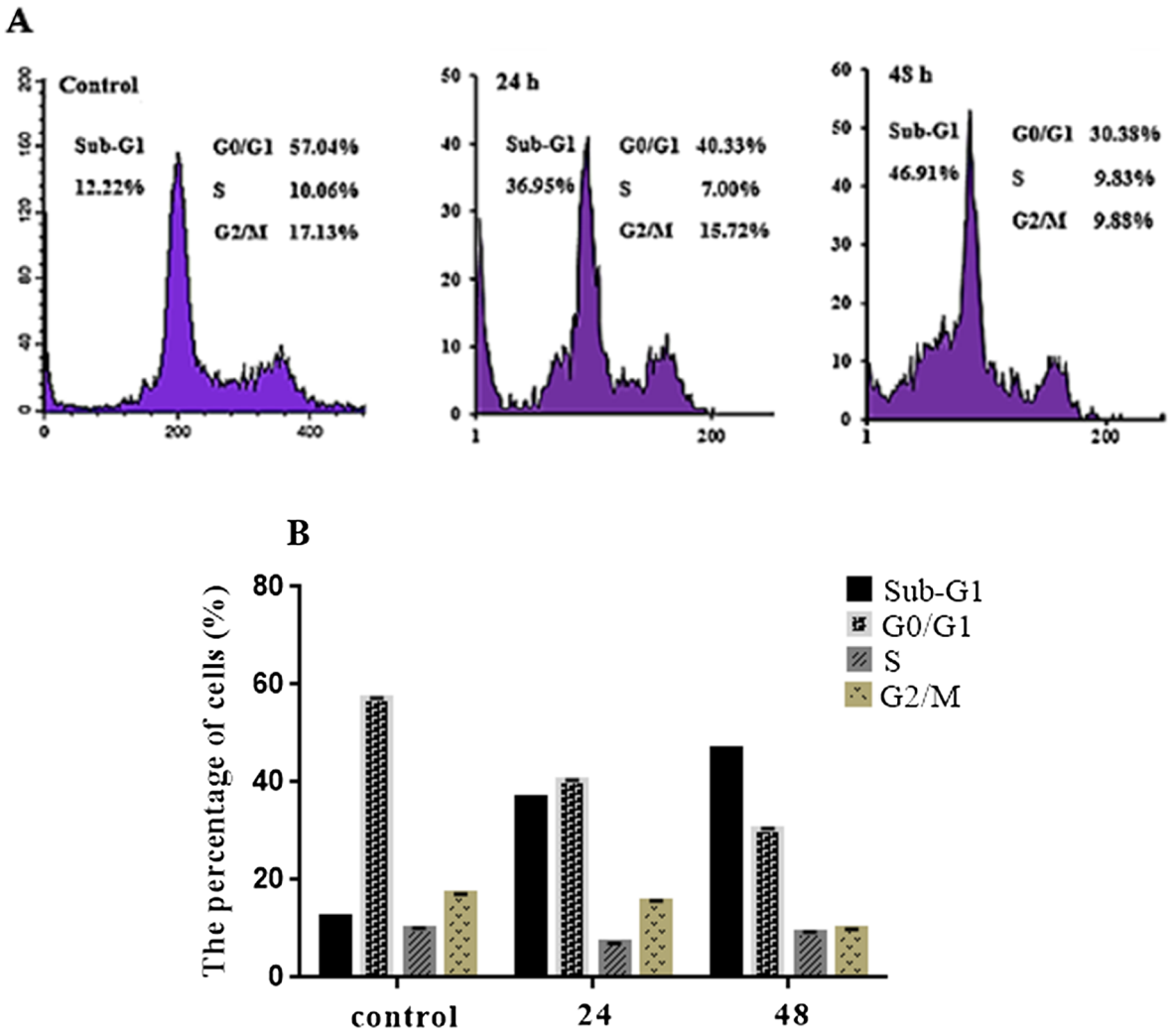

Fig. 5. 4c induces cell cycle arrest in HT-29 cells. (A) The cells were treated with the indicated concentrations (IC_{50} = 60 μM) of **4c** and harvested after 24 and 48 h. The cells were stained with propidium iodide (PI) and then the percentage of cells was calculated in each phase using flow cytometry. (B) The percentage of cells in sub-G1, G0/G1, S and G2/M. The results are expressed as mean ± S.D ($P < 0.05$).

apoptosis mediated by these receptors [53,54]. In most of tumor cells, treatments that up-regulate the levels of caspase-8 expression [53].

Caspases are a type of proteolytic enzymes doing important functions in programmed cell death. Caspase-3 is a key regulator in the initiation and execution pathways of apoptosis [52]. Based on the results of this study, elevation of caspase-3 expression was observed after treatment with 60 μM of 4c as compared with the untreated cells (respective control cells) (Fig. 7A). All gene expressions were normalized to GAPDH (reference gene). Based on Heo et al., sargachromonal E (SE) as a chromene derivative induces apoptosis via activation of caspase-3 in the human leukemia HL-60 cells [55]. In order to provide more evidence for the mechanism of 4c action in HT-29 cancer cells, the activation of caspase-8 and -9 which play important role in the regulation of extrinsic and intrinsic pathways, respectively, were analyzed. As shown in Fig. 7, the activation and up-regulation of caspase-8 and -9 after 48 h of incubation with IC_{50} value of 4c as a ligand was observed. As a result, chromene derivatives are a family of heterocycles compounds that play a key role in anti-proliferative and immunomodulatory responses.

Bcl-2, the anti-apoptotic Bcl-2 family member, prevents apoptotic cell death via binding to outer surface of mitochondria and sequestering Bax-like pro-apoptotic sub-family, namely Bax. The increased expression of Bcl-2 and reduced expression of Bax has been demonstrated in many drug-resistant tumor cells. The up-regulation of Bax and down-regulation of Bcl-2 could eliminate tumor cells by inducing apoptosis [50]. In the present study, up-regulation of Bax and down-regulation of Bcl-2 was evaluated after incubation of HT-29 cells with 4c (Fig. 7). It was recently recorded that 2-amino-4-(3-nitrophenyl)-3-cyano-7-(dimethyamino)-4*H*-chromene (3-NC) induces apoptosis by up-regulating Bax expression and down-regulating Bcl2 expression [47]. In addition, the increased ratio of Bax to Bcl-2 (Bax/Bcl-2) plays a significant role in collapse of mitochondrial membrane potential, which causes Cyt c release and cell death [50]. Thus, decreased Bcl-2 expression removes its inhibitory effect on Bax. This results in increased levels of Bax and activation of pro-caspase-9. Following caspase-9 activation the mitochondrial membrane potential, which is normally maintained by anti-

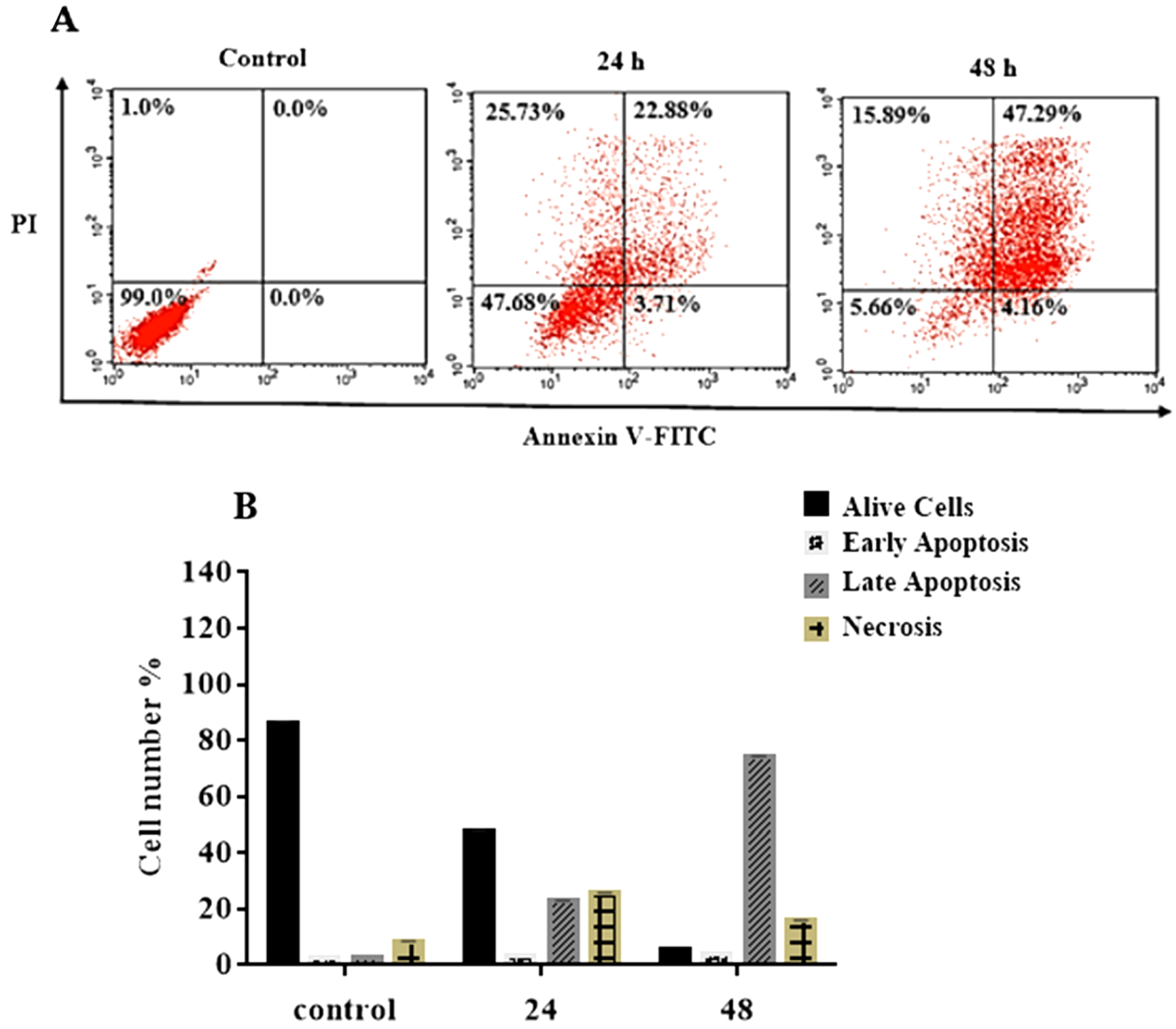

Fig. 6. Flow cytometry analysis of annexin-V and propidium iodide (PI) staining of apoptotic HT-29 cells treated by **4c** (60 μM). (A) The cells were treated with the indicated concentration of **4c** for 24 and 48 h. The percentage of cells was calculated in each phase using flow cytometry. (B) The percentage of cells in sub-G1, G0/G1, S and G2/M. The results are expressed as mean ± S.D ($P < 0.05$).

apoptotic Bcl-2 family members including Bcl-2 and Bcl-xl, becomes compromised. Thus, the ratio of Bax to Bcl-2 (Fig. 7F) is a critical way demonstrating the effect of 4c on HT-29 cells [47].

3.3. DNA binding activity of *4c*

3.3.1. UV–Vis spectroscopy

Electronic spectral studies is an easy and useful method for investigating the binding strength and the mode of small molecules binding with DNA [56]. Spectroscopic titration was carried out to study the binding probability of **4c** to ctDNA. Fig. 8A shows the absorption spectra of **4c** in the presence of adding various amounts of ctDNA. A hyperchromism was observed in the absorption spectra of **4c** in the peak area near 234 nm with the increasing concentration of DNA. Generally, the observed hyperchromism may result because of different non-covalent binding via outside the DNA double helix [57]. The absorption spectra of ctDNA in the presence of various amount of **4c** is displayed in Fig. 8B. In general, two main features of DNA spectra were "hyperchromic" and "hypochromic" effects, which arose owing to an alteration in its double helical structure [58,59]. Furthermore, Benesi-Hildebrand equation was used to obtain the binding constant (K) between **4c** and ctDNA [60]:

$$\frac{A_0}{A-A_0} = \frac{\varepsilon_G}{(\varepsilon_{H\text{-}G} - \varepsilon_G)} + \frac{\varepsilon_G}{(\varepsilon_{H\text{-}G} - \varepsilon_G)} \cdot \frac{1}{K[CT - DNA]} \quad (1)$$

where K is the apparent association constant, A_0 and A are the absorbance of the **4c** and **4c** -DNA complex, respectively. The ε_G and $\varepsilon_{H\text{-}G}$ are the absorption coefficients of the **4c** and the **4c**-DNA complex, respectively. The intrinsic binding constant (K) calculated for **4c** was $2.5 \times 10^3\ M^{-1}$ (Fig. 8C), which indicates that 4c binds to DNA through an outside binding manner.

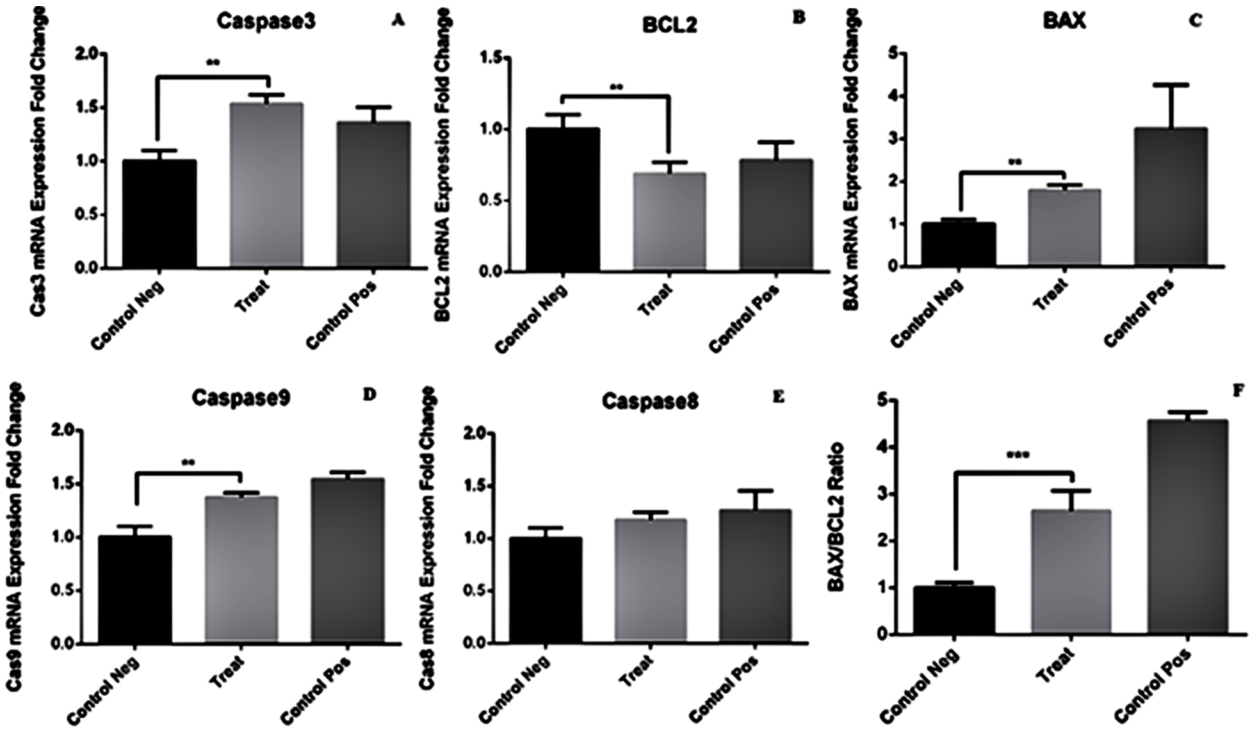

Fig. 7. Expression of apoptosis-related genes upon **4c** treatment. (A) RT-PCR analysis of caspse-3, (B) Bcl-2, (C) Bax, (D) caspase-9, (E) caspase-8 and (F) Bax/Bcl-2 ratio on HT-29 cells after 48 h treatment with the indicated concentration (IC_{50} value) of **4c**.

3.3.2. *Fluorescence quenching studies*

Fluorescence spectroscopy is one of the commonly suitable methods for studying agent-DNA interactions [59]. As, double helix DNA does not have intrinsic fluorescence, the fluorescence attribute of 4c was used here. The **4c** was excited in the absence and presence of ctDNA at 280 nm and the emission spectra was monitored (Fig. 9A). The fluorescence intensity of **4c** was gradually decreased with increasing concentration of ctDNA indicating the groove binding mode for the interaction between **4c** and ctDNA [61]. Due to the interaction of **4c** with ctDNA, the quenching constant was calculated. The ratio of fluorescence intensity (F_0/F) was plotted as a function of ctDNA concentration, in the presence and absence of ctDNA (Fig. 9B). K_{SV} (Stern-Volmer quenching constant) was evaluated from the slope of the Stern-Volmer plot (F_0/F vs. [DNA]) [58] and the K_{SV} value of 1.3×10^3 $Lmol^{-1}$ ($R^2 = 0.9848$) was calculated for **4c**. It was obvious that the quenching processes are of two types, static or dynamic. Bimolecular quenching constant (K_q) was calculated from the following Eq. (2) [58]:

$$K_q = K_{sv}/\tau_0 \quad (2)$$

where τ_0 is the lifetime of the fluorophore. The value of calculated K_q (1.3×10^{12} M^{-1} S^{-1}) in this study was higher than the value of the maximum scatter collision quenching constant (2.0×10^{10} M^{-1} S^{-1}) [62]. These data support a static quenching process. Moreover, Eq. (3) was applied to obtain the binding stoichiometry (n) and the binding constant (K_f) of **4c**-ctDNA [58]:

$$\log(F_0 - F)/\ F = \log K_f + n\log[Q] \quad (3)$$

where F_0 and F are the fluorescence emission intensities of **4c** in the absence and presence of ctDNA [Q], respectively. A Plot of log $[(F_0 - F)/F]$ vs. log [Q] was calculated and the intercept of this plot corresponds to log K (Fig. 9C). These results are displayed in Table 6. The low K_f (binding constant) value of **4c**, in contrast to intercalators [63,64], indicates that **4c** could interact with ctDNA through an outside binding mode.

3.3.3. *Viscosity measurements*

Viscosity measurements is a widely used hydrodynamic technique for studying the binding mode of DNA with small molecules [65]. The length of double helix DNA increases following the intercalation of planar ligands between adjacent base pairs, resulting in increment of DNA viscosity. On the other side, groove binding and electrostatic interactions, usually induce negligible change in the viscosity of DNA solution [57,66]. Fig. 10 shows the effects of different concentration of **4c** on the ctDNA viscosity. These results support the notion that **4c** interacts with ctDNA via a non-intercalative mode of binding.

4. Conclusion

In conclusion, here we reported on derivatives from the benzochromene family with apoptotic activity in HT-29 cells. **4c** was more active in comparison with the other compounds. We attribute the antiproliferative effect of this compound to several mechanisms including induction of apoptosis, flow cytometry method and expression of apoptosis- related genes. On the other hand, the binding properties of **4c** with double helix DNA was evaluated using spectral analysis and viscosity measurements. All the data presented here support the **4c**-DNA interactions through a non-intercalative mode. In summary, based on the promising findings presented here regarding the anticancer effects of **4c**, benzochromene derivatives are good candidates for further investigation of their mechanisms of action and features that make them remarkable as cancer therapeutic agents.

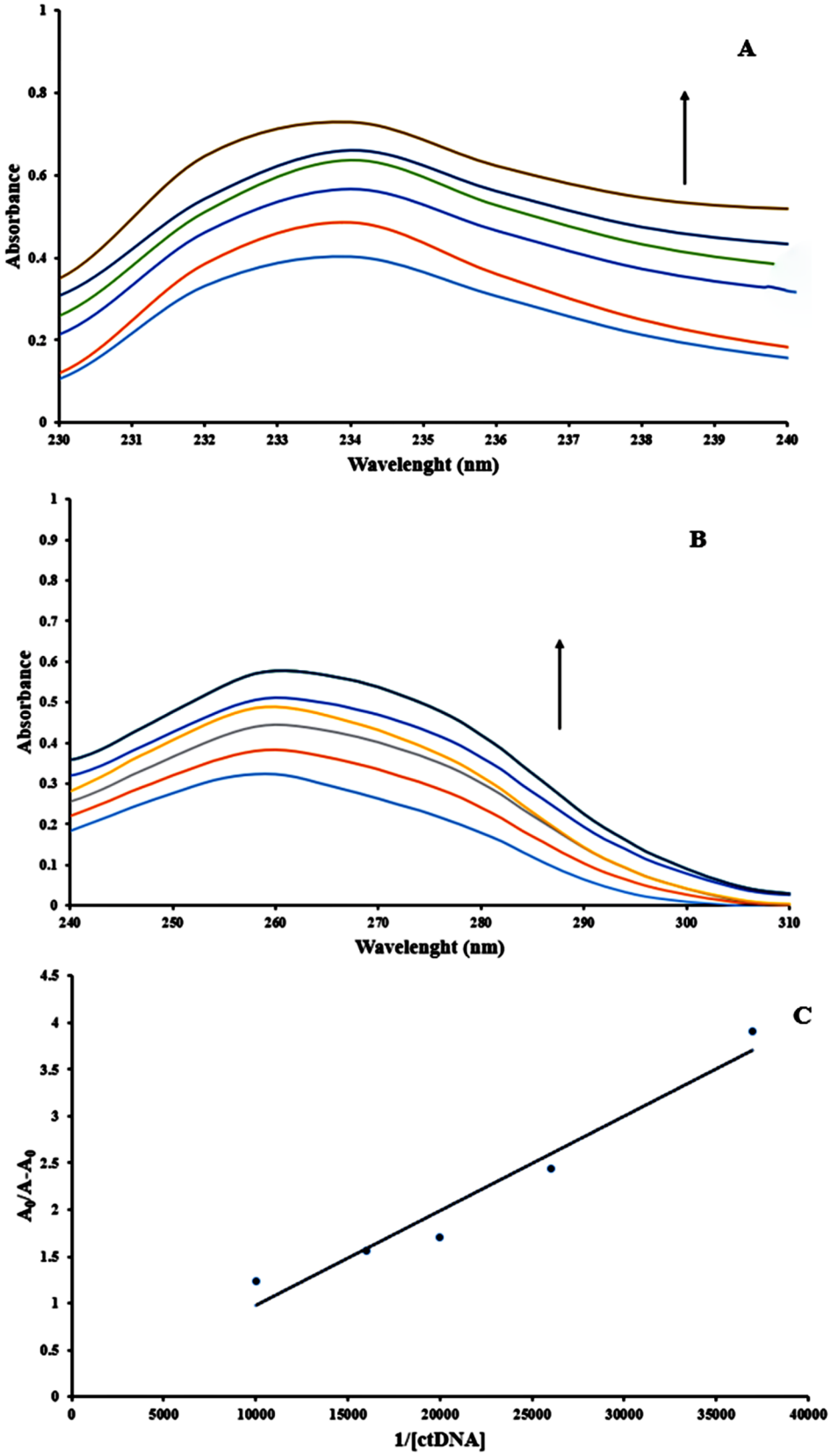

Fig. 8. (A) Absorption spectra: (A) **4c** (1.0×10^{-3} M) in the absence and presence of increasing amounts of ctDNA. [ctDNA] = ($2.7–10 \times 10^{-5}$ M). Arrow shows the absorbance change upon increasing ctDNA concentration. (B) ctDNA (5.0×10^{-5} M) in the absence or presence of increasing amounts of **4c**. ([**4c**] = (10–40 μM)) Arrow shows the absorbance changes upon increasing **4c** concentration. (C) Plot of $A_0/A–A_0$ vs 1/[ctDNA].

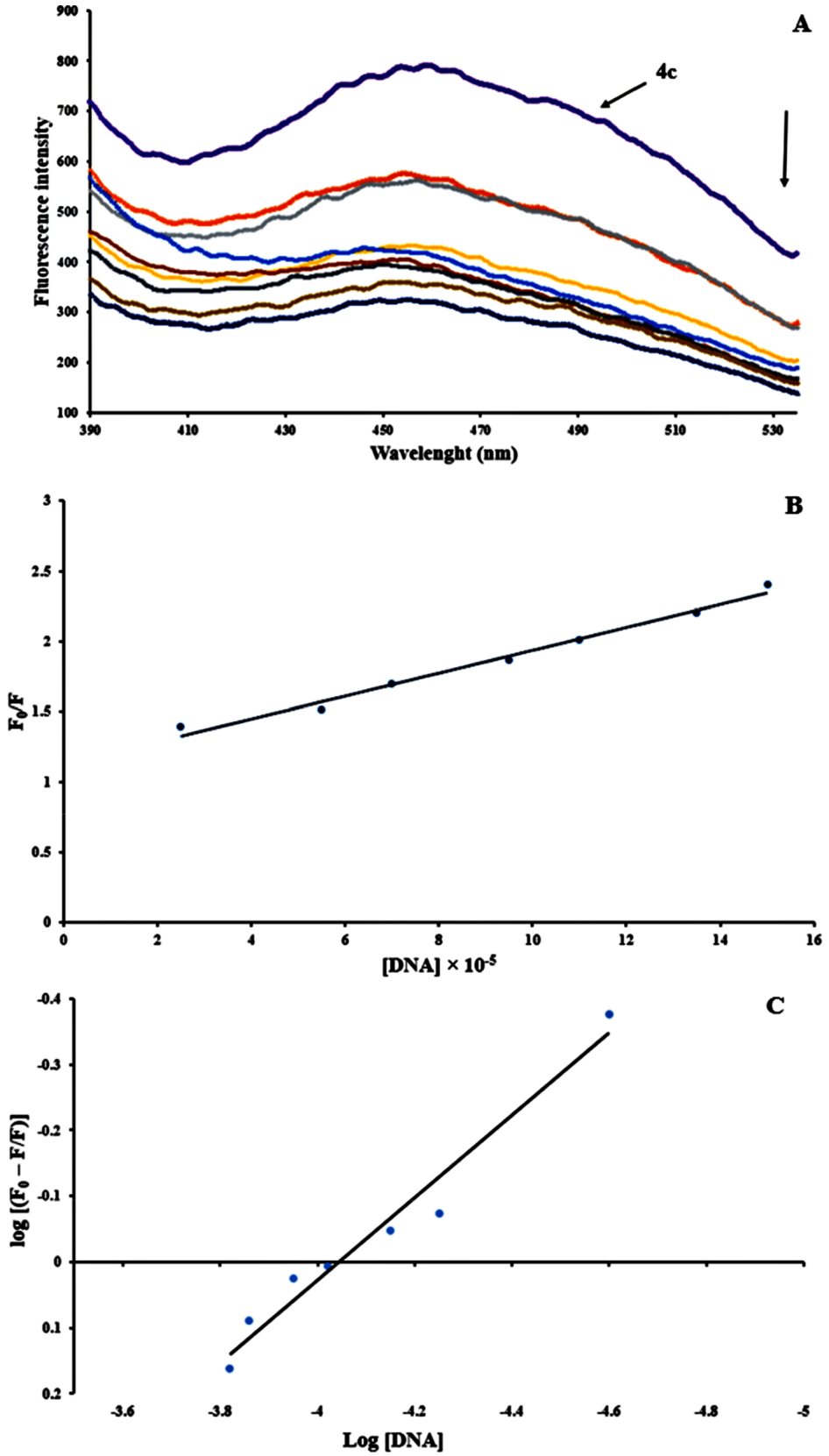

Fig. 9. (A) Emission spectra of **4c** (1.0×10^{-3} M) in the absence or presence of increasing amounts of ctDNA. [ctDNA] = ($2.5–15 \times 10^{-5}$ M). Arrow shows the emission intensity change upon increasing ctDNA concentration. (B) The Stern-Volmer plot of the **4c** fluorescence quenched by DNA. (C) Plot of log(F0/F)/F versus log [cT-DNA] to calculate the binding constant. The interaction of **4c** with cT-DNA was characterized using modified SternVolmer plot and the data obtained is shown in the respective table (Table 6).

Table 6
Parameters obtained using fluorescence study: Stern-Volmer constant, quenching constant, binding constant and number of binding between **4c**-DNA complex.

Compound	K_{SV} ($\times 10^4$) (L/mol)	Kq ($\times 10^{12}$) (L/mol per s)	K_f ($\times 10^4$)	n	R^2
4c	1.3	1.3	3.3	0.625	0.9848

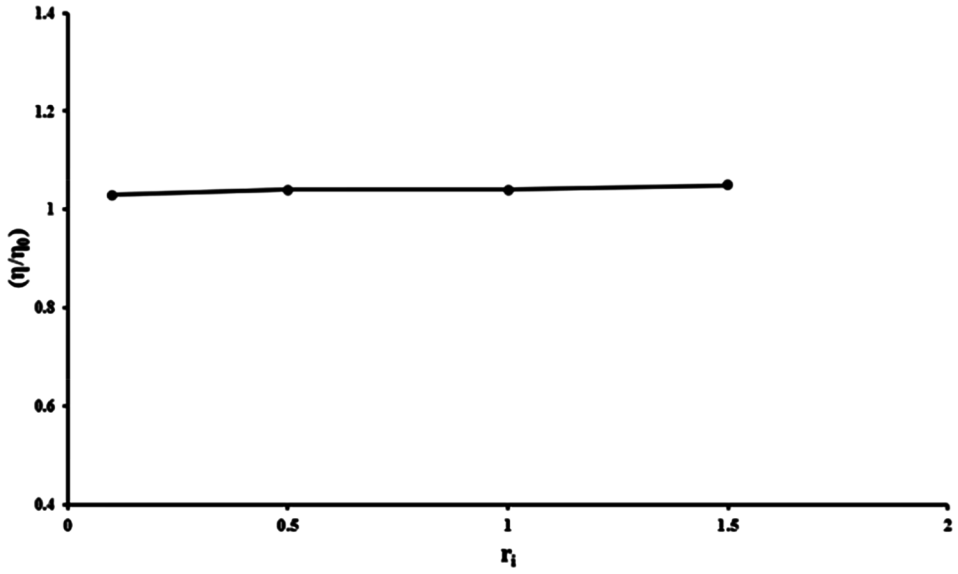

Fig. 10. Effect of increasing amounts of **4c** on the viscosity of ctDNA (5.0×10^{-5} M).

Acknowledgements

The authors are thankful to the foundation of this research by the Research Deputy of University of Tabriz, Tabriz, Iran.

Declaration of Competing Interests

No competing financial interests exist. The authors declare no conflict of interest.

References

[1] F.M. Roleira, C.L. Varela, S.C. Costa, E.J. Tavares-da-Silva, Phenolic derivatives from medicinal herbs and plant extracts: anticancer effects and synthetic approaches to modulate biological activity, Stud. Nat. Prod. Chem. 57 (2018) 115–156.
[2] O. Cheraghi, G. Dehghan, M. Mahdavi, R. Rahbarghazi, A. Rezabakhsh, H.N. Charoudeh, M. Iranshahi, S. Montazersaheb, Potent anti-angiogenic and cytotoxic effect of conferone on human colorectal adenocarcinoma HT-29 cells, Phytomedicine 23 (4) (2016) 398–405.
[3] S. Mignani, J. Rodrigues, H. Tomas, M. Zablocka, X. Shi, A.-M. Caminade, J.-P. Majoral, Dendrimers in combination with natural products and analogues as anti-cancer agents, Chem. Soc. Rev. 47 (2) (2018) 514–532.
[4] M. Ghasemian, M. Mahdavi, P. Zare, M.A.H. Feizi, Spiroquinazolinone-induced cytotoxicity and apoptosis in K562 human leukemia cells: alteration in expression levels of Bcl-2 and Bax, J. Toxicol. Sci. 40 (1) (2015) 115–126.
[5] R. Bai, W. Li, Y. Li, M. Ma, Y. Wang, J. Zhang, F. Hu, Cytotoxicity of two water-soluble polysaccharides from Codonopsis pilosula Nannf. var. modesta (Nannf.) LT Shen against human hepatocellular carcinoma HepG2 cells and its mechanism, Int. J. Biol. Macromol. 120 (2018) 1544–1550.
[6] J.M. Adams, S. Cory, The BCL-2 arbiters of apoptosis and their growing role as cancer targets, Cell Death Differ. 25 (1) (2018) 27.
[7] P.M. Waziri, R. Abdullah, R. Rosli, A.R. Omar, A.B. Abdul, N.K. Kassim, I. Malami, I.C. Etti, J.A.M. Sani, M.A.M. Lila, Clausenidin induces caspase 8-dependent apoptosis and suppresses production of VEGF in liver cancer cells, Asian Pac. J. Cancer Prev. 19 (4) (2018) 917.
[8] G. Greaves, M. Milani, D. Byrne, R. Carter, M. Butterworth, X. Luo, P. Eyers, G. Cohen, S. Varadarajan, PO-061 Bcl-2 family of proteins, bcl-xl and mcl-1, regulate apoptosis and cancer cell survival by different mechanisms, BMJ Publishing Group Limited, 2018.
[9] A. Keskin-Aktan, K.G. Akbulut, Ç. Yazici-Mutlu, G. Sonugur, M. Ocal, H. Akbulut, The effects of melatonin and curcumin on the expression of SIRT2, Bcl-2 and Bax in the hippocampus of adult rats, Brain Res. Bull. 137 (2018) 306–310.
[10] A. Russo, V. Cardile, A.C. Graziano, R. Avola, M. Bruno, D. Rigano, Involvement of Bax and Bcl-2 in induction of apoptosis by essential oils of three Lebanese salvia species in human prostate cancer cells, Int. J. Mol. Sci. 19 (1) (2018) 292.
[11] F.F. Alblewi, R.M. Okasha, Z.M. Hritani, H.M. Mohamed, M.A. El-Nassag, A.H. Halawa, A. Mora, A.M. Fouda, M.A. Assiri, A.-A.M. Al-Dies, Antiproliferative effect, cell cycle arrest and apoptosis generation of novel synthesized anticancer heterocyclic derivatives based 4*H*-benzo[*h*]chromene, Bioinorg. Chem. 87 (2019) 560–571.
[12] A. Foroumadi, G. Dehghan, A. Samzadeh-Kermani, F. Arabsorkhi, M. Sorkhi, A. Shafiee, M. Abdollahi, Synthesis and antioxidant activity of some 2-amino-4-aryl-3-cyano-7-(dimethylamino)-4*H*-chromenes, Asian J. Chem. 19 (2) (2007) 1391–1396.
[13] A.M. El-Agrody, A.M. Fouda, E.S.A. Khattab, Halogenated 2-amino-4*H*-benzo[*h*] chromene derivatives as antitumor agents and the relationship between lipophilicity and antitumor activity, Med. Chem. Res. 26 (4) (2017) 691–700.
[14] G. Mata, J. Rodrigues, N. Gamboa, K. Charris, G. Lobo, M. Monasterios, M. Avendano, M. Lein, K. Jung, C. Abramjuk, Synthesis, antiproliferative, and antiangiogenic activities of benzochromene and benzoquinoline derivatives on prostate cancer in vitro, Lett. Drug Des. Discov. 14 (4) (2017) 398–413.
[15] M.F. Dehkordi, G. Dehghan, M. Mahdavi, M.A. Hosseinpour, DNA binding study of dihydropyrano [3,4-C] chromene derivative by some spectroscopic techniques, J. Rep. Pharm. Sci. 5 (2) (2016) 80–82.
[16] M.F. Dehkordi, G. Dehghan, M. Mahdavi, M.A.H. Feizi, Multispectral studies of DNA binding, antioxidant and cytotoxic activities of a new pyranochromene derivative, Spectrochim. Acta, Part A 145 (2015) 353–359.
[17] M. Costa, T.A. Dias, A. Brito, F. Proenca, Biological importance of structurally diversified chromenes, Eur. J. Med. Chem. 1 (23) (2016) 487–507.
[18] S.A. Patil, R. Patil, L.M. Pfeffer, D.D. Miller, Chromenes: potential new chemotherapeutic agents for cancer, Future Med. Chem. 5 (14) (2013) 1647–1660.
[19] H.K. Abd El-Mawgoud, H.A.M. Radwan, F. El-Mariah, A.M. El-Agrody, Synthesis characterization, biological activity of novel 1H-benzo [f]-chromene and 12*H*-benzo[*f*]chromeno[2,3-d]pyrimidine derivatives, Lett. Drug Des. Discov. 15 (8) (2018) 857–865.
[20] C. Bingi, N.R. Emmadi, M. Chennapuram, Y. Poornachandra, C.G. Kumar, J.B. Nanubolu, K. Atmakur, One-pot catalyst free synthesis of novel kojic acid tagged 2-aryl/alkyl substituted-4H-chromenes and evaluation of their antimicrobial and anti-biofilm activities, Bioorg. Med. Chem. lett. 25 (9) (2015) 1915–1919.
[21] J.-J. Chen, J.-Y. Cho, T.-L. Hwang, I.-S. Chen, Benzoic acid derivatives, acetophenones, and anti-inflammatory constituents from Melicope semecarpifolia, J.

Nat. Prod. 71 (1) (2007) 71–75.
[22] W. Gregor, G. Grabner, C. Adelwöhrer, T. Rosenau, L. Gille, Antioxidant properties of natural and synthetic chromanol derivatives: study by fast kinetics and electron spin resonance spectroscopy, J. Org. Chem. 70 (9) (2005) 3472–3483.
[23] E. Abbaspour-Gilandeh, S.C. Azimi, Li (OHCH2CH2NH2)(CF3OAC): a novel and homogeneous acidic ionic liquid catalyst for efficient synthesis of 2-amino-4H-chromene derivatives, Iran. J. Catal. 4 (4) (2014) 281–288.
[24] W. Kemnitzer, J. Drewe, S. Jiang, H. Zhang, Y. Wang, J. Zhao, S. Jia, J. Herich, D. Labreque, R. Storer, Discovery of 4-Aryl-4 H-chromenes as a new series of apoptosis inducers using a cell-and caspase-based high-throughput screening assay. 1. structure− activity relationships of the 4-Aryl group, J. Med. Chem. 47 (25) (2004) 6299–6310.
[25] T.H. Afifi, R.M. Okasha, H.E. Ahmed, J. Ilaš, T. Saleh, A.S. Abd-El-Aziz, Structure-activity relationships and molecular docking studies of chromene and chromene based azo chromophores: a novel series of potent antimicrobial and anticancer agents, EXCLI J. 16 (2017) 868.
[26] A. Kheirollahi, M. Pordeli, M. Safavi, S. Mashkouri, M.R. Naimi-Jamal, S.K. Ardestani, Cytotoxic and apoptotic effects of synthetic benzochromene derivatives on human cancer cell lines, Naunyn-Schmiedeberg's Arch. Pharmacol. 387 (12) (2014) 1199–1208.
[27] A.H. Halawa, A.M. Fouda, A.-A.M. Al-Dies, A.M. El-Agrody, Synthesis, biological evaluation and molecular docking studies of 4Hbenzo [h] chromenes, 7*H*-benzo[*h*] chromeno[2,3-d]pyrimidines as antitumor agents, Lett. Drug Des. Discov. 13 (1) (2016) 77–88.
[28] N. Pravin, V. Devaraji, N. Raman, Targeting protein kinase and DNA molecules by diimine–phthalate complexes in antiproliferative activity, Int. J. Biol. Macromol. 79 (2015) 837–855.
[29] M. Mehdipour, G. Dehghan, R. Yekta, M. Hanifeh Ahagh, M. Mahdavi, Z. Ghasemi, Z. Fathi, DNA-binding affinity, cytotoxicity, apoptosis, cell cycle inhibition and molecular docking studies of a new stilbene derivative, Nucleos., Nucleot. Nucl. Acids (2019) 1–18.
[30] M. Muti, M. Muti, Electrochemical monitoring of the interaction between anticancer drug and DNA in the presence of antioxidant, Talanta 178 (2018) 1033–1039.
[31] E. Payami, H. Abbasi, E.S. Yazdchi, K.D. Safa, R. Teimuri-Mofrad, Synthesis and study of electrochemical behavior of new 4-ferrocenylbutylamine derivatives, Org. Chem. (2018) 431–441.
[32] R. Teimuri-Mofrad, M. Gholamhosseini-Nazari, E. Payami, S. Esmati, Ferrocene-tagged ionic liquid stabilized on silica-coated magnetic nanoparticles: efficient catalyst for the synthesis of 2-amino-3-cyano-4*H*-pyran derivatives under solvent-free conditions, Appl. Organomet. Chem. 32 (1) (2018) e3955.
[33] R. Teimuri-Mofrad, M. Gholamhosseini-Nazari, E. Payami, S. Esmati, Novel ferrocene-based ionic liquid supported on silica nanoparticles as efficient catalyst for synthesis of naphthopyran derivatives, Res. Chem. Intermed. 43 (12) (2017) 7105–7118.
[34] E.A. Queiroz, Z.B. Fortes, M.A. da Cunha, H.K. Sarilmiser, A.M.B. Dekker, E.T. Öner, R.F. Dekker, N. Khaper, Levan promotes antiproliferative and pro-apoptotic effects in MCF-7 breast cancer cells mediated by oxidative stress, Int. J. Biol. Macromol. 102 (2017) 565–570.
[35] A. Bahuguna, I. Khan, V.K. Bajpai, S.C. Kang, MTT assay to evaluate the cytotoxic potential of a drug, J. Pharmacol. 12 (2) (2017) 115–118.
[36] R. Dhanyakrishnan, M.C. Sunitha, B. Prakash Kumar, S. Sandya, K.G. Nevin, Morphological and molecular effects of phenolic extract from coconut kernel on human prostate cancer cell growth in vitro, J. Nutr. Metab. 11 (1) (2018) 21–36.
[37] N. Shobeiri, M. Rashedi, F. Mosaffa, A. Zarghi, M. Ghandadi, A. Ghasemi, R. Ghodsi, Synthesis and biological evaluation of quinoline analogues of flavones as potential anticancer agents and tubulin polymerization inhibitors, Eur. J. Med. Chem. 114 (2016) 14–23.
[38] R. Noelanders, K. Vleminckx, Cell cycle analysis of the embryonic brain of fluorescent reporter Xenopus tropicalis by flow cytometry, Xenopus (2018) 243–250.
[39] E.J. Vanzyl, K.R. Rick, A.B. Blackmore, E.M. MacFarlane, B.C. McKay, Flow cytometric analysis identifies changes in S and M phases as novel cell cycle alterations induced by the splicing inhibitor isoginkgetin, PloS one 13 (1) (2018) e0191178.
[40] M.A. Sugimoto, J.P. Vago, M.M. Teixeira, L.P. Sousa, Annexin A1 and the resolution of inflammation: modulation of neutrophil recruitment, apoptosis, and clearance, J. Immunol. Res. 2016 (2016).
[41] M. Dehkhodaei, M. Sahihi, H.A. Rudbari, F. Momenbeik, DNA and HSA interaction of Vanadium (IV), Copper (II), and Zinc (II) complexes derived from an asymmetric bidentate Schiff-base ligand: multi spectroscopic, viscosity measurements, molecular docking, and ONIOM studies, J. Biol. Inorg. Chem. 23 (2) (2018) 181–192.
[42] S.A. Abdelatef, M.T. El-Saadi, N.H. Amin, A.H. Abdelazeem, H.A. Omar, K.R. Abdellatif, Design, synthesis and anticancer evaluation of novel spirobenzo [h] chromene and spirochromane derivatives with dual EGFR and B-RAF inhibitory activities, Eur. J. Med. Chem. 150 (2018) 567–578.
[43] R. Okasha, F. Alblewi, T. Afifi, A. Naqvi, A. Fouda, A.-A. Al-Dies, A. El-Agrody, Design of new benzo[*h*]chromene derivatives: antitumor activities and structure-activity relationships of the 2, 3-positions and fused rings at the 2, 3-positions, Molecules 22 (3) (2017) 479.
[44] H.M. Mohamed, A.M. Fouda, E.S. Khattab, A.M. El-Agrody, T.H. Afifi, Synthesis, in-vitro cytotoxicity of 1*H*-benzo[*f*]chromene derivatives and structure–activity relationships of the 1-aryl group and 9-position, Z. Naturforsch. 72 (5–6) (2017) 161–171.
[45] T.D. Duensing, S.R. Watson, Assessment of Apoptosis (Programmed Cell Death) by Flow Cytometry, Cold Spring Harbor Protocols 2018(1) (2018) pdb. prot093807.
[46] O. Belzile, X. Huang, J. Gong, J. Carlson, A.J. Schroit, R.A. Brekken, B.D. Freimark, Antibody targeting of phosphatidylserine for the detection and immunotherapy of cancer, ImmunoTargets Ther. 7 (2018) 7.
[47] M.H. Naseri, M. Mahdavi, J. Davoodi, S.H. Tackallou, M. Goudarzvand, S.H. Neishabouri, Up regulation of Bax and down regulation of Bcl2 during 3-NC mediated apoptosis in human cancer cells, Cancer Cell Int. 15 (1) (2015) 55.
[48] Z.A. Radi, Z.S. Stewart, S.P. O'Neil, Accidental and programmed cell death in investigative and toxicologic pathology, Curr. Protoc. Toxicol. 76 (1) (2018) e51.
[49] M.C. Pearce, J.T. Gamble, P.R. Kopparapu, E.F. O'Donnell, M.J. Mueller, H.S. Jang, J.A. Greenwood, A.C. Satterthwait, R.L. Tanguay, X.-K. Zhang, Induction of apoptosis and suppression of tumor growth by Nur77-derived Bcl-2 converting peptide in chemoresistant lung cancer cells, Oncotarget 9 (40) (2018) 26072.
[50] D. Kumar, S. Haldar, M. Gorain, S. Kumar, F.A. Mulani, A.S. Yadav, L. Miele, H.V. Thulasiram, G.C. Kundu, Epoxyazadiradione suppresses breast tumor growth through mitochondrial depolarization and caspase-dependent apoptosis by targeting PI3K/Akt pathway, BMC Cancer 18 (1) (2018) 52.
[51] J.-W. Shin, S.-B. Kwon, Y. Bak, S.-K. Lee, D.-Y. Yoon, BCI induces apoptosis via generation of reactive oxygen species and activation of intrinsic mitochondrial pathway in H1299 lung cancer cells, Sci. China: Life Sci. 61 (10) (2018) 1243–1253.
[52] M. Tsoli, J. Liu, L. Franshaw, H. Shen, C. Cheng, M. Jung, S. Joshi, A. Ehteda, A. Khan, A. Montero-Carcabosso, Dual targeting of mitochondrial function and mTOR pathway as a therapeutic strategy for diffuse intrinsic pontine glioma, Oncotarget 9 (7) (2018) 7541.
[53] C. Ruiz-Ruiz, C.R. de Almodóvar, A. Rodríguez, G. Ortiz-Ferrón, J.M. Redondo, A. López-Rivas, The up-regulation of human caspase-8 by interferon-γ in breast tumor cells requires the induction and action of the transcription factor interferon regulatory factor-1, J. BioL. Chem. 279 (19) (2004) 19712–19720.
[54] W. Hu, J.J. Kavanagh, Anticancer therapy targeting the apoptotic pathway, Lancet Oncol. 4 (12) (2003) 721–729.
[55] S.-J. Heo, K.-N. Kim, W.-J. Yoon, C. Oh, Y.-U. Choi, A. Affan, Y.-J. Lee, H.-S. Lee, D.-H. Kang, Chromene induces apoptosis via caspase-3 activation in human leukemia HL-60 cells, Food Chem. Toxicol. 49 (9) (2011) 1998–2004.
[56] Y. Rahman, S. Afrin, M.A. Husain, T. Sarwar, A. Ali, M. Tabish, Unravelling the interaction of pirenzepine, a gastrointestinal disorder drug, with calf thymus DNA: an in vitro and molecular modelling study, Arch. Biochem. Biophys. 625 (2017) 1–12.
[57] F.A. Qais, K. Abdullah, M.M. Alam, I. Naseem, I. Ahmad, Interaction of capsaicin with calf thymus DNA: a multi-spectroscopic and molecular modelling study, Int. J. Biol. Macromol. 97 (2017) 392–402.
[58] M. Parveen, F. Ahmad, A.M. Malla, M.S. Khan, S.U. Rehman, M. Tabish, M.R. Silva, P.P. Silva, Structure elucidation and DNA binding specificity of natural compounds from Cassia siamea leaves: a biophysical approach, J. Photochem. Photobiol., B 159 (2016) 218–228.
[59] N. Shahabadi, S. Fatahi, M. Maghsudi, Synthesis of a new Pt (II) complex containing valganciclovir drug and calf-thymus DNA interaction study using multi-spectroscopic methods, J. Coord. Chem. 71 (2) (2018) 258–270.
[60] H.A. Benesi, J. Hildebrand, A spectrophotometric investigation of the interaction of iodine with aromatic hydrocarbons, J. Am. Chem. Soc. 71 (8) (1949) 2703–2707.
[61] H.N. KiranKumar, H.G. RohitKumar, G.M. Advirao, D.N.A. Synthesis, binding and cytotoxic activity of pyrimido [4′, 5′: 4, 5] thieno (2, 3-b) quinoline with 9-hydroxy-4-(3-diethylaminopropylamino) and 8-methoxy-4-(3-diethylaminopropylamino) substitutions, J. Photochem. Photobiol., B 178 (2018) 1–9.
[62] W.R. Ware, Oxygen quenching of fluorescence in solution: an experimental study of the diffusion process, J. Phys. Chem. 66 (3) (1962) 455–458.
[63] A. Kocak, H. Yilmaz, O. Faiz, O. Andac, Experimental and theoretical studies on Cu (II) complex of N, N′-disalicylidene-2, 3-diaminopyridine ligand reveal indirect evidence for DNA intercalation, Polyhedron 104 (2016) 106–115.
[64] A. Tarushi, C. Kakoulidou, C.P. Raptopoulou, V. Psycharis, D.P. Kessissoglou, I. Zoi, A.N. Papadopoulos, G. Psomas, Zinc complexes of diflunisal: synthesis, characterization, structure, antioxidant activity, and in vitro and in silico study of the interaction with DNA and albumins, J. Inorg. Biochem. 170 (2017) 85–97.
[65] R. Vijimalar, G.L. Rose, A.T. Bhosan, J. Joseph, Synthesis, structural characterization, anti-microbial and DNA binding studies of novel schiff base metal (Ii) complexes derived from isoniazid and 2-(4-Nitro-Phenyl)-2h-Isoquinolin-1-One (2018).
[66] J.-H. Shi, K.-L. Zhou, Y.-Y. Lou, D.-Q. Pan, Multi-spectroscopic and molecular docking studies on the interaction of darunavir, a HIV protease inhibitor with calf thymus DNA, Spectrochim. Acta, Part A 193 (2018) 14–22.
[67] M. Tajbakhsh, M. Kariminasab, H. Alinezhad, R. Hosseinzadeh, P. Rezaee, M. Tajbakhsh, H.J. Gazvini, M.A. Amiri, Nano silica-bonded aminoethylpiperazine: a highly efficient and reusable heterogeneous catalyst for the synthesis of 4H-chromene and 12H-chromeno [2, 3-d] pyrimidine derivatives, J. Iran. Chem. Soc. 12 (8) (2015) 1405–1414.